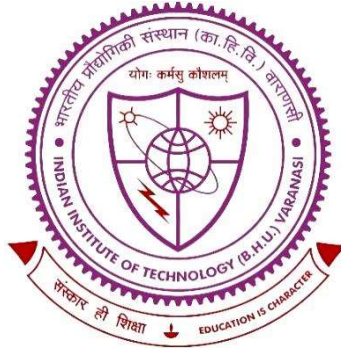


Spectroscopy and Learning-based Image processing
for
Cardiac Diagnosis



Thesis submitted in partial fulfillment

for the Award of Degree

Doctor of Philosophy

by

Taresh Sarvesh Sharan

SCHOOL OF BIOMEDICAL ENGINEERING

INDIAN INSTITUTE OF TECHNOLOGY

(BANARAS HINDU UNIVERSITY)

VARANASI – 221005

16021005

January 2022

CERTIFICATE

It is certified that the work contained in the thesis titled “**Spectroscopy and Learning-based Image processing for Cardiac diagnosis**” by “**Taresh Sarvesh Sharan**” has been carried out under my supervision and this work has not been submitted elsewhere for a degree.

It is further certified that the student has fulfilled all the requirements of Comprehensive Examination, Candidacy and SOTA for the award of Ph.D. Degree.

(Dr. Shiru Sharma)
Supervisor
Associate Professor,
School of Biomedical Engineering,
Indian Institute of Technology (BHU),
Varanasi - 221005, (U.P.), India

(Dr. Marshal)
Co-Supervisor
Associate Professor,
School of Biomedical Engineering,
Indian Institute of Technology (BHU),
Varanasi - 221005, (U.P.), India

DECLARATION BY THE CANDIDATE

I, Taresh Sarvesh Sharan, certify that the work embodied in this Ph.D. thesis is my own bona fide work and carried out by me under the supervision of Dr. Shiru Sharma, and Dr. Marshal from **July 2016 to January 2022** at the School of Biomedical Engineering, Indian Institute of Technology (BHU), Varanasi. The matter embodied in this thesis has not been submitted for the award of any other degree/diploma.

I declare that I have faithfully acknowledged and given credits to the research workers wherever their work has been cited in my work in this thesis. I further declare that I have not willfully copied any other's work, paragraphs, text, data, results, etc., reported in journals, books, magazines, reports dissertations, theses, etc., or available at websites and have not included them in this thesis and have not cited as my own work.

Taresh Sarvesh Sharan

Date:
Place:

Signature of the Student
(Taresh Sarvesh Sharan)

CERTIFICATE BY THE SUPERVISOR

It is certified that the above statement made by the student is correct to the best of my/our knowledge.

(Dr. Shiru Sharma)
Supervisor
Associate Professor,
School of Biomedical Engg.,
Indian Institute of Technology (BHU),
Varanasi - 221005, (U.P.), India

(Dr. Marshal)
Co-Supervisor
Associate Professor,
School of Biomedical Engg.,
Indian Institute of Technology (BHU),
Varanasi - 221005, (U.P.), India

(Prof. P. K. Roy)
Coordinator
School of Biomedical Engg., Indian Institute of Technology (BHU),
Varanasi - 221005, (U.P.), India

COPYRIGHT TRANSFER CERTIFICATE

Title of the Thesis: Spectroscopy and learning-based Image processing for cardiac diagnosis

Name of the Student: Taresh Sarvesh Sharan

Copyright Transfer

The undersigned hereby assigns to the Indian Institute of Technology (BHU), Varanasi all rights under copyright that may exist in and for the above thesis submitted for the award of the Doctor of Philosophy.

Date:

Place:

Taresh Sarvesh Sharan

Signature of the Student

(Taresh Sarvesh Sharan)

Note: However, the author may reproduce or authorize others to reproduce material extracted verbatim from the thesis or derivative of the thesis for author's personal use provided that the source and the Institute's copyright notice are indicated.

**DEDICATED
TO**

*Maa
&
Papa*

Table of Contents

List of Figures.....	<i>xi</i>
List of Tables	<i>xiv</i>
List of Abbreviations	<i>xvi</i>
Perface.....	<i>xvii</i>

Part –I BACKGROUND

Chapter 1

Introduction: Cardiac Diagnostic: Spectroscopy and Image aspect	3
1.1 Brief Ovrview of cardiac disease and diagnostics	3
1.2 Outline of Spectroscopy based cardiac diagnosis.....	4
1.3 Outline of Image-based cardiac diagnosis	7
1.4 Problems with Spectroscopy and Image-based cardiac diagnosis.....	9
1.5 Thesis Objectives.....	10
1.6 Thesis Contribution	10
1.7 Thesis Organization	11
References.....	13

Chapter 2

Spectroscopy in Cardiac Diagnosis	17
2.1 Cardiac biomarker.....	17
2.2 Spectroscopic methods.....	18
2.3 Spectrocy-based Troponin’s detection	18
2.4 Spectrocy-based CRP detection	20
2.5 Spectrocy-based BNP/NT-proBNP and TNF- α detection	21
2.6 Spectrocy-based myoglobin detection	22
2.7 Other cardiac biomarker detection methods.....	23
References.....	24

Chapter 3

Learning-based image processing for cardiac diagnosis	29
3.1 Classical image segmentation appoches	30
3.1.1 K-Means Clustering approach.....	30
3.1.2 Random walker approach	31

3.1.3 Region growing approach	32
3.2 Deep learning approaches	33
References	36

Part – II SPECTROSCOPY IN CARDIAC DIAGNOSIS

Chapter 4

Fabrication of a fiber scanner probe for spectroscopy	43
4.1 Introduction.....	44
4.2 material and Method	48
4.2.1 Piezoelectric tube	48
4.2.2 3-D printed mounts	50
4.2.3 Fiber cantilever	50
4.2.4 LabVIEWcontrol program	52
4.3 Results and Discussion.....	54
4.4 Conclusion	57
References.....	58

Chapter 5

Spectroscopy and signal processing in cardiac diagnostic	60
Abstract.....	60
5.1 Introduction.....	61
5.1.1 Cardiac biomarker detection.....	61
5.1.2 Spectroscopy signal processing.....	62
5.2 Material and Methods	64
5.3 Result and Discussion	68
5.3.1 Biomarker detection	68
5.3.2 Spectroscopy signal processing.....	70
5.3.2.1 Spike removal from spectroscopy signal.....	70
5.3.2.2 Denoising of noisy spectrum model.....	72
5.4 Conclusion	75
References.....	76

Part – III USING LEARNING BASED APPROACH FOR CARDIAC MRI PROCESSING

Chapter 6 Evaluation of a weakly supervised learning-based segmentation method for cardiac images.....	82
Abstract.....	82
6.1 Introduction.....	83
6.2 Method	86
6.2.1 Seed region growing based segmentation	88
6.2.2 K-Means clustering-based segmentation	89
6.2.3 Random walker-based segmentation	90
6.3 Experiments.....	96
6.3.1 Datasets.....	91
6.3.2 Pre-processing	92
6.3.3 Training protocol	92
6.3.2 Loss function and evaluation metrics.....	93
6.4 Results	94
6.4.1 Comparison of all segmentation methods.....	94
6.4.2 Model training with fewer images	95
6.5 Discussion.....	103
6.6 Conclusion	105
References.....	105

Chapter 7	
Transfer learning and modified U-Net-based segmentation method on normal and noisy cardiac images	110
Abstract.....	110
7.1 Introduction.....	111
7.2 Method	116
7.2.1 Transfer learning algorithm	116
7.2.1.1 Feature pyramid Network.....	116
7.2.1.2 U-Net	117
7.2.2 Modified U-Net algorithm	116
7.3 Experiments	124
7.3.1 Transfer learning algorithm	124
7.3.2 Modified U-Net algorithm	126
7.4 Results	128
7.4.1 Transfer learning algorithm	128

7.4.2 Modified U-Net algorithm	136
7.5 Discussion	124
7.5.1 Transfer learning algorithm	124
7.5.2 Modified U-Net algorithm	116
7.6 Conclusion	116
References.....	117

Part – IV CLOSURE

Chapter 8	
Summary and Conclusion	121
Chapter 9	
Future Scope of Work	123
References.....	124

Part – V ACCOMPLISHMENTS

Publications (Journal Articles)	127
Publications (Conference Articles).....	127
Conferences and Workshops.....	128
Other Publications (During Doctoral Studies)	128

LIST OF FIGURES

Figure No.	Figure description	Page No.
Figure 4.1	General overview of endoscope (a) Schematic of complete system (b) Fabricated microendoscope (c) Solid works cross view of microendoscope showing internal structures	47
Figure 4.2	AutoCAD model (a) Complete probe (b) lower mount having a groove for PZT wire take out (c) front mount used for coupling PZT with fiber cantilever (d) Actual fiber probe.	49
Figure 4.3	GUI for the custom-made signal acquisition and image formation algorithm developed using LabVIEW	52
Figure 4.4	Stability study of fabricated endoscope (a) Scanning pattern (b) Short-term distribution of single acquisition point in XY plane (c) long term stability of fiber tip (d) Long term stability of four randomly selected points	55
Figure 5.1	Cardiac Troponin I structure and its interactive surroundings	62
Figure 5.2	TEM Images of (a) Gold Nanoparticles (b) cTnI conjugated AuNPs and (c) SAD pattern	69
Figure 5.3	UV-Visible spectra (a) Gold Nanoparticles (b) Gold nano particles and cTnI conjugated Gold nanoparticles.	70
Figure 5.4	UV-Visible spectra of cTnI conjugated gold nanoparticles for three different concentrations.	70
Figure 5.5	FTIR of Gold nanoparticle and cTnI conjugated gold nanoparticle	71
Figure 5.6	(a) Raman signal with simulated spikes (b) Level 1 detail coefficient of DDDTCWT (c) Level 1 approximate coefficient of Double Density dual-tree complex wavelet transforms (d) Despiked Raman signal	72
Figure 5.7	(a) Xanthan Raman Spectrum (b) Glucose Raman Spectrum (c) Xanthan Raman spectrum noise model (d) Glucose Raman spectrum noise model (e) Double Density dual-tree complex wavelet transform denoised Xanthan Raman spectrum (f) Double Density dual-tree complex wavelet transform denoised Glucose Raman spectrum	74
Figure 5.8	(a) Variation of Signal to noise ratio of the denoised signal using different methods as the noise level is varied (b) Variation of Root mean square error of the denoised signal using different methods as the noise level is varied	75
Figure 6.1	Graphical representation of Methods	87

Figure 6.2	Figure 6.2: Segmentation result for unsupervised methods compared to supervised training (a) Original image (b) Mask (c) Seed Region Growing segmentation (d) Random Walker Segmentation (e) K Means Clustering Segmentation (f) Autoencoder supervised learning	94
Figure 6.3	Segmentation result for Seed Region Growing method (a) & (g) Image (b) & (h) Target (c) & (i) Segmentation result for All images (d) & (j) Segmentation result for Degree I (e) & (k) Segmentation result for Degree II (f) & (l) Segmentation result for Degree III	95
Figure 6.4	Segmentation result for Random Walker method (a) & (g) Image (b) & (h) Target (c) & (i) Segmentation result for All images (d) & (j) Segmentation result for Degree I (e) & (k) Segmentation result for Degree II (f) & (l) Segmentation result for Degree III	96
Figure 6.5	segmentation result for K-Means Clustering method (a) & (g) Image (b) & (h) Target (c) & (i) Segmentation result for All images (d) & (j) Segmentation result for Degree I (e) & (k) Segmentation result for Degree II (f) & (l) Segmentation result for Degree III	96
Figure 6.6	Error plot for Dataset 1 in (a) Dice score of Seed Region Growing (b) Dice score of Random walker (c) Dice score of K-Means Clustering (d) Jaccard Index of Seed Region Growing (e) Jaccard Index of Random walker (f) Jaccard Index of K-Means Clustering	100
Figure 6.7	Error plot for Dataset 2 in (a) Dice score of Seed Region Growing (b) Dice score of Random walker (c) Dice score of K-Means Clustering (d) Jaccard Index of Seed Region Growing (e) Jaccard Index of Random walker (f) Jaccard Index of K-Means Clustering	101
Figure 7.1	Feature Pyramid Network generalized architecture with bottom-up and top-down pathways	115
Figure 7.2	U-Net generalized architecture with contractive and expansive paths	116
Figure 7.3	(a) Depth wise Separable block (b) Architecture of the proposed network (c) Noise stifler Block	117
Figure 7.4	End-diastolic FPN network (a) Original Image (b) Ground Truth (c) FPN with DenseNet encoder Prediction (d) FPN with ResNet encoder Prediction (e) FPN with VGG Prediction	125
Figure 7.5	End-diastolic U-NET network (a) Original Image (b) Ground Truth (c) U-NET DenseNet Prediction (d) UNET with ResNet encoder Prediction (e) U-NET with encoder VGG Prediction	126
Figure 7.6	End-diastolic U-NET network (a) Original Image (b) Ground Truth (c) U-NET DenseNet Prediction (d) UNET with ResNet encoder Prediction (e) U-NET with encoder VGG Prediction	126

Figure 7.7	End-Systolic FPN network (a) Original Image (b) Ground Truth (c) FPN with DenseNet encoder Prediction (d) FPN with ResNet encoder Prediction (e) FPN with VGG encoder Prediction	127
Figure 7.8	End-Systolic U-NET network (a) Original Image (b) Ground Truth (c) UNET with DenseNet encoder Prediction (d) U-NET with ResNet encoder Prediction (e) U-NET with VGG encoder Prediction	127
Figure 7.9	Evaluation metrics for different networks for End-systolic Phase(a) Sensitivity (b) Precision (c) MCC (d) Specificity	128
Figure 7.10	Segmentation results of ACDC dataset. First column (a)-(s) presents the mask of the image being segmented, first row (b)-(f) presents the original image and noisy version (1%,3%,5% and 7%) of the original image. Second, third and fourth rows presents the segmented results for Seg-Net (h)-(l), U-net (n)-(r) and proposed network (t)-(x). Second, third, fourth, fifth and sixth column presents the segmented results for original (h)-(t), 1% (i)-(u), 3% (j)-(v), 5% (k)-(w) and 7%(l)-(x) noise corrupted images.	131
Figure 7.11	Segmentation results of SCD dataset. First column (a)-(s) presents the mask of the image being segmented, first row (b)-(f) presents the original image and noisy version (1%,3%,5% and 7%) of the original image. Second, third and fourth rows presents the segmented results for Seg-Net (h)-(l), U-net (n)-(r) and proposed network (t)-(x). Second, third, fourth, fifth and sixth column presents the segmented results for original (h)-(t), 1% (i)-(u), 3% (j)-(v), 5% (k)-(w) and 7%(l)-(x) noise corrupted images.	133
Figure 7.12	Comparison of Specificity, Sensitivity and Precision for the networks. First to fifth bars of each metric presents results for original image, 1%, 3%, 5% and 7% noise corrupted images respectively	134
Figure 7.13	Layout plan of Ablation study	135

LIST OF TABLES

Table No.	Table description	Page No.
Table 2.1	Cardiac troponin detection biosensors based on SERS	19
Table 5.1	Signal to noise ratio and Root mean square error for test signals	73
Table 5.2	Signal to noise ratio and Root means square error for actual Raman signals	75
Table 6.1	Segmentation metrics for different methods in dataset 1; Mean (\pm Std)	96
Table 6.2	Segmentation Metrics for Seed Region growing method for all images and lesser images in dataset 1; Mean (\pm Std)	97
Table 6.3	Segmentation Metrics for Random Walker method for all images and lesser images in dataset 1; Mean (\pm Std)	98
Table 6.4	Segmentation Metrics for K Means method for all images and lesser images in dataset 1; Mean (\pm Std)	98
Table 6.5	Segmentation Metrics for different Methods in dataset 2; Mean (\pm Std)	98
Table 6.6	Segmentation Metrics for Seed Region Grow method for all images and lesser images in dataset 2; Mean (\pm Std)	99
Table 6.7	Segmentation Metrics for Random Walker method for all images and lesser images in dataset 2; Mean (\pm Std)	99
Table 6.8	Segmentation Metrics for K Means method for all images and lesser images in dataset 2; Mean (\pm Std)	100
Table 7.1	Dice Score for End-Diastolic and End-Systolic cardiac phases for different models	128
Table 7.2	Jaccard Index for End-Diastolic and End-Systolic cardiac phase for different models	128
Table 7.3	Comparison of overall mean of dice score of three classes for different methods	129
Table 7.4	Comparison of mean Hausdorff distance for different classes	130
Table 7.5	Evaluation Metrics Comparison for ACDC dataset	132
Table 7.6	Evaluation Metrics Comparison for SCD dataset	133
Table 7.7	Comparison results of segmentation	134

Table 7.8	Ablation Study: Evaluation Metrics Comparison of SCD dataset for noise free original images	135
Table 7.9	Ablation Study: Evaluation Metric Comparison of SCD dataset for 7% noise corrupted images	136

LIST OF ABBREVIATIONS

MRI	Magnetic Resonance Imaging
CMRI	Cardiac Magnetic Resonance Imaging
MSE	Mean Squared Error
SSIM	Structural Similarity Index Measure
GD	Gradient Descent
FCN	Fully Convolutional Network
CNN	Convolutional Neural Network
ROI	Region of Interest
CPU	Central Processing Unit
GPU	Graphics Processing Unit
CVDs	Cardiovascular diseases
ECG	Electrocardiogram
PCG	Phonocardiogram
CRP	C-reactive protein
SERS	Surface enhanced Raman spectroscopy
SPR	Surface plasmon resonance
cTnI	Cardiac troponin I
ELISA	Enzyme-linked immunosorbent assay
CT	Computed tomography
ROI	Region of interest
FCN	Feature pyramid network
PAN	Projective adversarial network
DCAN	Deep contour network
RELU	Rectified exponential linear unit
SELU	Scaled exponential linear unit
CLAHE	Contrast limited adaptive histogram enhancement
ACDC	Automatic cardiac diagnosis challenge

PREFACE

The major cause of death worldwide is cardiovascular diseases (CVDs). In 2016, approximately 17.9 million people died because of CVDs which represents 31% of the global death. Out of these, 85% of deaths are due to heart attack or stroke. 75% of deaths due to CVDs occur in mid-income and low-income countries. One in 4 deaths in India is now because of CVDs with ischemic heart disease and stroke, responsible for >80% of burden on healthcare system. Recognition of CVDs is the first and most important step in the treatment and management of the patients by the healthcare system. Timely diagnosis of cardiovascular disease plays a vital role in the effective management of high-risk patients. Early diagnosis of heart disease not only helps in providing adequate life-saving therapeutic intervention but also reduces the load on the healthcare system. Increased risk of death due to CVDs demands for accurate, rapid, sensitive, and reliable, affordable detection systems.

Several diagnostic modalities are developed for heart function analysis like biomarker monitoring. Broadly, cardiac function analysis modalities can be subdivided into Image-based systems, Signal based systems, and biomarker-based systems. Imaging techniques include but are not limited to Cardiac Magnetic Resonance Imaging (CMRI), Echocardiography, and Computed tomography. Signal Processing techniques include Phonocardiography (PCG) and Electrocardiography (ECG) while Biomarker based techniques include detection of cardiac-specific biomarkers detection like troponins (cTnI, cTnT, Myoglobin, etc.). Biomarkers specific to the heart are established to be identifiers of CVDs whose concentration varies as the physiological and pathological condition of the cardiac environment varies.

Several biomarkers are identified for CVDs within blood serum or plasma such as Cardiac Troponins, NT-proBNP, C-reactive protein (CRP), Myoglobin, etc. Several techniques have been developed for the early diagnosis of stroke and other CVDs. Techniques such as surface plasmon

resonance (SPR), immunoassays, enzyme-linked immunosorbent assay (ELISA), surface-enhanced Raman spectroscopy (SERS), field-effect transistor-based methods, and liquid chromatography are commonly used for the quantification of biomarkers. Drawbacks of these methods include sample-specific preparation, long processing time, and the requirement of central laboratories. Recently, the main focus has been on point-of-care tests (POCT) for portability, small sample size, fast detection, and high accuracy.

In first phase of the work, biomarker-based detection of CVDS is explored using spectroscopy methods. Biomarkers are small molecules that can be quantified and help in the prognosis of the heart condition. Concentration above a certain value for biomarkers represents the changes of occurring of cardiac event in near future or certain heart condition is developed recently. Several spectroscopic methods had been used by different research groups still limitations exist in the method. Major limitations are:

- Method specific and tedious sample preparation
- Long processing and result time
- Requirement of central lab
- Lack of standardization
- Lack of prognosis capabilities and lower detection of limit

Spectroscopy based methods are proved to require no sample preparation method with faster results, and higher detection accuracy. UV-Vis, Raman, and Fourier transform infrared Spectroscopy is mainly investigated in this work for label-free detection of cardiac biomarker Cardiac Troponin I (cTnI). UV-Vis spectroscopy provided a SPR quenching phenomenon when biomarker is conjugated with gold nanoparticles. The 530 nm SPR peak of gold nanoparticles vanished as the concentration of cTnI is increased above certain level. The conjugation of cTnI

with gold nanoparticles are further visualized using TEM images. The initial Raman signal for gold conjugated cTnI provided a hint of low concentration detection of the biomarker using multivariate signal processing but the results were initial and no conclusive inference can be drawn. The occurrence of global pandemic and shutdown of the institutes caused the postponement of the project and no further verification can be carried out as sample procurement and instrument handling is highly affected by the global situation. Further, the application of double density dual tree complex wavelet transform is also evaluated and observed that the method is not only able to remove the spikes from the spectroscopy signals but also have better denoising capabilities compared to other state-of-the-art denoising methods.

In the second phase of this work, Image based cardiac diagnosis is investigated mainly focusing on cardiac MR images. Cardiac Magnetic resonance imaging is considered the gold standard for non-invasive cardiac function analysis due to its 3D capabilities and high spatiotemporal resolution. It had been already proved to be an invaluable tool in the diagnosis of complex cardiomyopathies. Cardiac Magnetic resonance not only helps in the visualization of cardiac anatomy but also allows to know the functional behavior of the heart. Clinical implications of cardiac MRI are:

- Quantify coronary blood flow
- Measurement of ventricular volumes, wall thickness, and other parameters.
- Quantify myocardial infarction size.
- Myocardial viability
- Measure blood flow in the myocardium

Cardiac function analysis provides several information related to heart structure and helps in the diagnosis of several pathological conditions like hyper cardiomyopathy. But to accurately

extract this information from cardiac function analysis-based modalities especially MRI, accurate segmentation is of the utmost importance. Despite several hardware and software advancements in recent years, several limitations exist like the requirement of ground truth, Image intensity and contrast inhomogeneity, and others. Major difficulties in Image-based diagnosis, regarding MRI, are as:

- Poor contrast between myocardium and surrounding structures
- Brightness heterogeneities in LV and RV chamber due to blood flow
- Presence of trabeculae and papillary muscles with intensity similar to the myocardium
- Inherent noise due to motion and heart dynamics
- Shape and intensity variability of heart structures
- Presence of banding artifact

These problems in the cardiac MR images makes the physicians difficult to do inference regarding the clinical conditions. To augment them, automated segmentation of the images is carried out which is further used to extract features to classify the patient as a normal or abnormal. To do so, accurate segmentation of the images is required for which a transfer learning-based method, a modified U-Net network, and a cascaded model is proposed. Results showed that the methods proposed are well-performed and the cascaded model paved a way to go from supervised learning to unsupervised learning thus removing the need of ground truth which is a hectic task.

The principal objective of the thesis is to improve methods of cardiac diagnostic by improving two of the most used aspects: Image-based diagnosis and Spectroscopy based diagnosis. In this view, this thesis aims to full fill the following objectives like design and optimization of Raman probe for Cardiac troponin I detection, validation of the use of spectroscopic methods in Cardiac troponin I detection, spectral signal processing to extract more accurate and quantitative

information from the signal, development of an algorithm for more accurate segmentation of CMRI to improve feature extraction for diagnosis of the cardiac pathological condition, and to pave a way towards unsupervised segmentation of cardiac images to exploit the availability of vast unannotated biomedical image data for better diagnosis.

Part - I

BACKGROUND

